

## **Lightweighting a fire-truck frame: CAD–FEA benchmarking of SS304, IS 2062, and Al 7075-T6 for stiffness, safety, mass, and cost**

Akhilesh Ranjan<sup>1</sup>, Viraz Wadia<sup>2</sup>, Narendra Khatri<sup>2\*</sup>, K Abhimanyu Kumar Patro<sup>2</sup>, Mandeep Singh<sup>3</sup>, Vineet Pandey<sup>4</sup>, Sumit Pokhriyal<sup>5,6</sup>

<sup>1</sup>Department of Physics, Manipal Institute of Technology, Manipal Academy of Higher Education, Manipal-576104, India; ak.ranjan@manipal.edu (A.R.).

<sup>2</sup>Department of Mechatronics, Manipal Institute of Technology, Manipal Academy of Higher Education, Manipal-576104, India; viraz.wadia@learner.manipal.edu (V.W.) narendra.khatri@manipal.edu (N.K.) abhimanyu.patro@manipal.edu (K.P.).

<sup>3</sup>Department of Mechanical Engineering, University of Engineering & Management, Jaipur- 303807, Rajasthan, India; mnndpsingh898@gmail.com (M.S.).

<sup>4</sup>School of Automation, Banasthali Vidyapith, Niwai-304022, Tonk, Rajasthan, India; vineetresearch84@gmail.com (V.P.).

<sup>5</sup>Department of Physics, Graphic Era Hill University, Dehradun, India; pl.sumit@gmail.com (S.P.).

<sup>6</sup>Graphic Era Deemed to be University, Dehradun, Uttarakhand, India.

**Abstract:** Reducing structural mass without compromising safety is central to improving the efficiency and operational capability of heavy emergency vehicles. This study evaluates three widely deployable materials, Stainless Steel (SS 304), Mild Steel (IS 2062), and Aluminum 7075-T6, for a fire-truck superstructure frame using a controlled CAD–FEA protocol. A full-scale ladder-frame was modeled in SolidWorks and analyzed in ANSYS (static structural) under identical boundary conditions representative of service loads (fixed runners on chassis rails, gravity, and a 100 kN tank load distributed to supports). Key performance indicators included maximum/average total deformation, maximum principal stress, factor of safety (FoS), frame mass, and indicative material cost. Mild steel achieved the lowest deformation (12.81 mm; average 0.186 mm) and a FoS of 6.28; SS 304 was comparable in deformation (13.295 mm; average 0.193 mm) with FoS 5.23. Aluminum 7075-T6 showed higher elastic deformation (36.185 mm; average 0.523 mm) but delivered the highest FoS (7.16) and a 62% mass reduction (300 kg vs 790 kg for SS). Maximum principal stresses were nearly identical across materials (~28.65 MPa), remaining well below their respective yields (SS 304 ~292 MPa; IS 2062 ~460 MPa; Al 7075-T6 ~500–540 MPa). Indicative material costs (₹/kg) favored mild steel (60–80) over stainless steel (150–200) and aluminum (400–500). The results quantify clear trade-offs: mild steel offers cost-optimal stiffness; aluminum provides transformative mass savings and safety margin; stainless steel suits higher-corrosion contexts with a weight penalty. These findings support material selection pathways aligned to fleet priorities (capex vs payload/efficiency) and motivate follow-on fatigue/dynamic analyses for duty-cycle certification.

**Keywords:** Aluminium alloy, Factor of safety, Finite element analysis, Fire truck frame, Material selection, Structural deformation.

### **1. Introduction**

The modern automotive sector has been continuously driven by the dual imperatives of improving vehicle performance and minimizing environmental impact. Among the various strategies employed, vehicle weight reduction has consistently emerged as one of the most effective approaches to enhance fuel efficiency, reduce emissions, and improve operational capability. In heavy-duty vehicles such as fire trucks, which carry large payloads and are expected to perform under extreme emergency conditions, the challenge of balancing structural integrity with lightweighting becomes even more

critical.

Numerous studies have established a direct link between a vehicle's unladen mass and its fuel consumption, demonstrating that weight reduction remains one of the simplest and most impactful strategies to achieve operational efficiency. For instance, Galos et al. [1] examined the energy savings achieved by lowering the empty weight of heavy goods vehicle (HGV) trailers, revealing significant reductions in both operational costs and carbon emissions. Although the study focused on HGVs, its conclusions are directly relevant to fire trucks due to their similar mass and load-bearing characteristics. With stringent emissions targets such as the UK's 80% reduction by 2050 compared to 1990 levels, the transport sector faces increasing pressure to adopt lighter, more efficient materials and structural solutions [1].

Wang et al. [2] highlight that achieving vehicle lightweighting requires a multi-pronged strategy, including the development of stronger yet lighter materials, the refinement of manufacturing processes, and advanced structural design through methods like topology optimization [2]. These approaches are increasingly supported by Integrated Computational Materials Engineering (ICME), which accelerates the development of tailored materials. However, practical challenges persist, especially in hybrid structures where materials such as steel and aluminum must be joined efficiently and remain recyclable [3].

The effectiveness of material substitution has been extensively documented, with materials such as magnesium, aluminum alloys, carbon fibre composites, and advanced high-strength steels achieving mass reductions ranging from 15% to 75% compared to conventional mild steel, albeit at varying cost levels. For example, aluminum alloys typically reduce weight by 40–60% at 1.3–2 times the relative cost, while carbon fibre composites offer even greater weight savings but at substantially higher costs [2, 3].

Taub et al. [4] further emphasized three principal pathways for weight reduction: lightweight material substitution, design optimization, and vehicle downsizing [4]. While the exact relationship between weight and fuel consumption is complex, empirical evidence suggests that a 10% reduction in vehicle weight typically results in a 6–8% decrease in fuel consumption [5, 6]. This relationship is particularly significant for fire trucks, where lower weight directly translates to increased payload capacity, improved maneuverability, and reduced operational costs, all critical during emergency response scenarios.

Traditionally, stainless steel 304 has been widely used in fire truck frame construction due to its corrosion resistance, durability, and strength [7]. However, its high density ( $\sim 8 \text{ g/cm}^3$ ) contributes to increased vehicle mass, limiting payload capacity and fuel efficiency. Aluminum alloys, in contrast, provide a compelling alternative due to their low density ( $\sim 2.8 \text{ g/cm}^3$ ), high strength-to-weight ratio, good corrosion resistance, and manufacturability [8]. Over the past few decades, the automotive industry has increasingly shifted toward aluminum, making it the second most used material after steel [9].

Padmanabhan et al. [10] examined various materials for truck chassis and noted that structural steel provided better resistance factors and lower deflection compared to unspecified aluminum alloys, although the study did not account for real-world dynamic stresses and cost implications. Padmanabhan et al. [10]. Agarwal and Mthembu [11] and Agarwal and Mthembu [12] explored advanced materials such as metal matrix composites (MMC), achieving up to 70% chassis weight reduction, but raised concerns regarding deformation and safety factors [11, 12]. Similarly, Dhabliya et al. [13] used finite element analysis (FEA) to evaluate steel and carbon fibre composites for fire truck chassis, finding that carbon fibre provided superior stiffness and fatigue resistance but at significantly higher cost and manufacturing complexity [13, 14].

Tisza [15] discussed and compared steel and aluminium in automotive structures, noting that steel remains preferred for its strength and crashworthiness, whereas aluminium offers clear advantages in weight reduction and corrosion resistance, albeit with lower absolute strength and higher joining complexity [15]. In practice, a hybrid material strategy is often adopted to exploit the

unique advantages of each material [16].

Given these advancements in material science and structural design, the fire truck manufacturing sector has lagged in adopting newer lightweight materials for primary frame structures. Fire trucks continue to rely largely on stainless steel frames, which, while robust, compromise fuel efficiency and payload due to their weight. The application of FE-based structural analysis provides a systematic and cost-efficient means to evaluate alternative materials under simulated real-world loading conditions. By developing a 3D CAD model in SolidWorks and analyzing it through ANSYS, it becomes possible to compare key performance indicators such as deformation, stress distribution, factor of safety, and weight for different candidate materials under identical conditions.

This study, therefore, investigates the structural performance of stainless steel (SS 304), mild steel (IS 2062), and aluminium alloy (Al 7075-T6) for a fire truck frame. Each material presents distinct trade-offs in terms of weight, cost, mechanical performance, corrosion resistance, and manufacturability. Through a combination of modelling and simulation, the research aims to identify an optimal balance that meets safety, efficiency, and economic requirements.

While extensive literature exists on lightweighting strategies in general automotive applications, specific investigations into material substitution for fire truck frame structures remain limited. Previous studies either focus on passenger or freight vehicles, neglect dynamic loading conditions unique to fire trucks, or fail to provide comparative structural analyses across multiple conventional and advanced materials. There is a lack of systematic, quantitative evaluation of conventional steels, aluminum alloys, and their alternatives under realistic emergency-response loading scenarios. The objectives of the study are (i) to evaluate and compare the structural performance of stainless steel, mild steel, and aluminum alloy fire truck frames under simulated operational loads. (ii) to quantify deformation, stress distribution, factor of safety, and weight for each material using CAD-FEA techniques. (iii) to identify an optimal material selection strategy balancing safety, cost, and weight reduction for fire truck frames.

## 2. Materials and Methods

### 2.1. Materials

#### 2.1.1. Vehicle Structural

The fire truck superstructure is mounted on a ladder-frame chassis that carries the water tank, hose reel, and pump modules, equipment compartments, and crew cabin. The frame must (i) distribute static and dynamic loads safely to the chassis rails, (ii) resist torsion during cornering and uneven terrain, and (iii) sustain repeated service cycles with minimal fatigue damage. Key design priorities, therefore, include structural integrity, fatigue life, corrosion resistance, and maintainability, while containing mass to preserve payload and fuel efficiency.



**Figure 1.**  
Schematic of the ladder-frame chassis.

### 2.1.2. Candidate Frame Materials

Three widely available metal systems aligned with fleet manufacturability and cost realities were down-selected for comparative assessment: Stainless Steel (SS 304). Austenitic stainless steel with excellent general corrosion resistance and robust ductility. Its density penalizes mass; chloride-rich service may require higher-molybdenum grades for pitting resistance. Mild Steel (IS 2062). Low-carbon structural steel, highly weldable and cost-effective with good yield strength, requires coatings or galvanization to manage corrosion. Aluminum Alloy (Al 7075-T6). High strength-to-weight alloy (Zn-Mg system) with attractive fatigue resistance and very low density; joining and raw-material cost need consideration.

**Table 1.**  
Material properties used in simulation (engineering data).

Property	SS 304	Al 7075-T6	IS 2062 (Mild Steel)
Density ( $\text{g}\cdot\text{cm}^{-3}$ )	7.86	2.81	7.85
Ultimate tensile strength, UTS (MPa)	685	570	560
Yield strength, $\sigma_Y$ (MPa)	292	505	460
Young's modulus, E (GPa)	207	72	205
Poisson's ratio (-)	0.27	0.33	0.285
Shear modulus, G (GPa)	81	26.9	80

## 3. Methods

### 3.1. CAD Development and Design Controls

A full-scale 3D CAD representation of the superstructure was created in SolidWorks using hollow square sections to reflect production intent (pipes/channels/angles/sheets) and authentic joint geometry where it affects stiffness. Dimensional fidelity was maintained for interchangeability and manufacturability (cut list, BOM, and jig references). Design considerations include weight, ergonomics, strength/FoS, ease of assembly/disassembly, material availability, and compliance with applicable regulations.

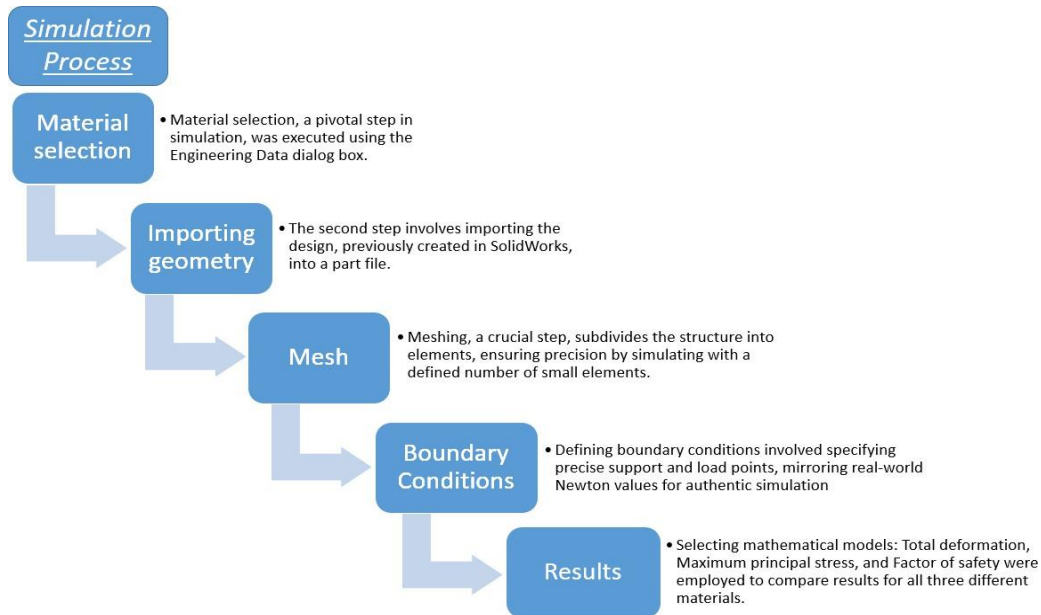


**Figure 2.**

CAD pipeline from concept to production: parametric skeleton, weldments, and interface definitions.

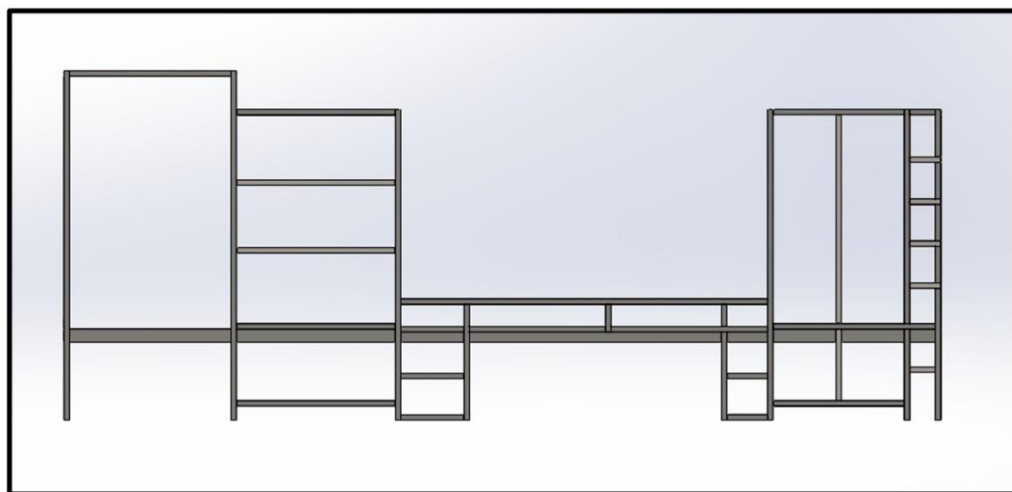


**Figure 3.**

CAD model side elevation with major members and mounting points annotated.

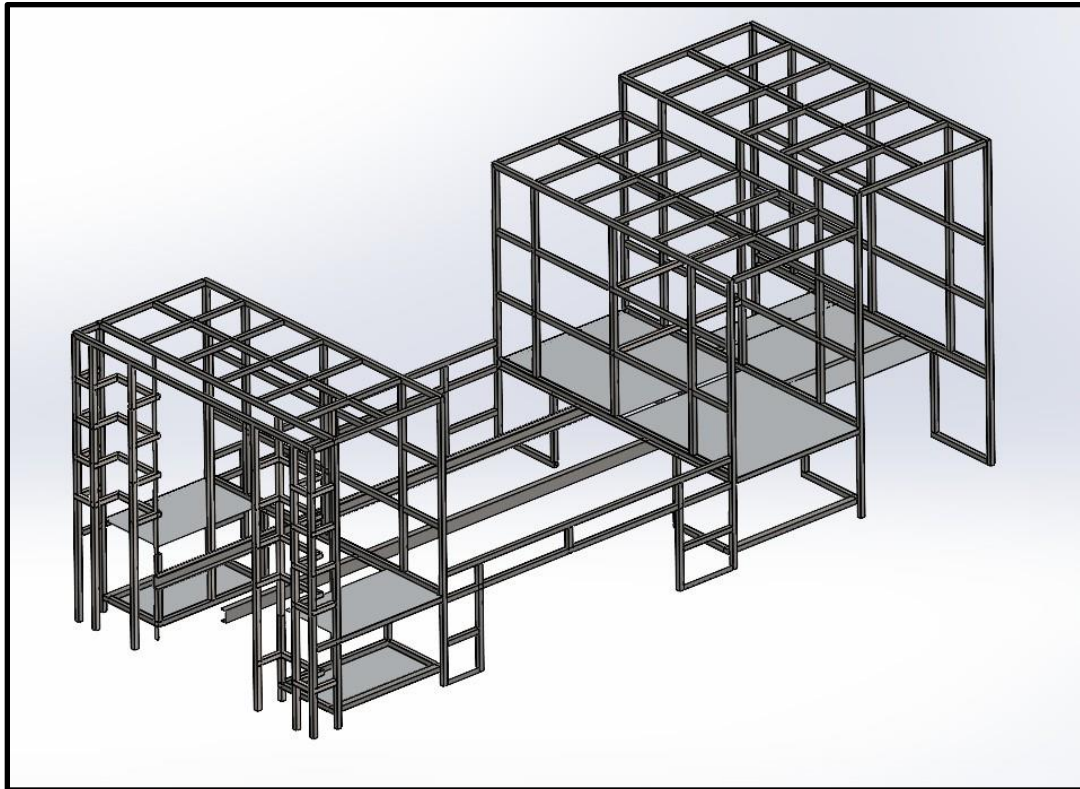


**Figure 4.**  
CAD model, isometric view showing cross-member layout and runner attachment.

**Table 2.**  
Principal geometric/vehicle parameters.

Parameter	Value
Overall length × width × height (mm)	6350 × 2520 × 2535
Structural tube OD × thickness (mm)	40 × 2 (square)
Runner support	Continuous on chassis rails (fixed support in FEA)
CAD-estimated frame mass (SS/IS/Al)	790 760 / 300 kg

### 3.1.1. Finite Element Modelling

All structural evaluations were performed using ANSYS (Static Structural) with identical geometry and load cases for the three material substitutions to isolate material effects. Element type and mesh: The frame was meshed with 3D solid elements (tet/hexa mix as auto-generated by ANSYS). A target element size of 30 mm was selected after sensitivity checks against the smallest flat (40 mm tube face), balancing accuracy and runtime. Local mesh refinement was applied near chassis interfaces, tank supports, and overhangs to capture stress gradients.

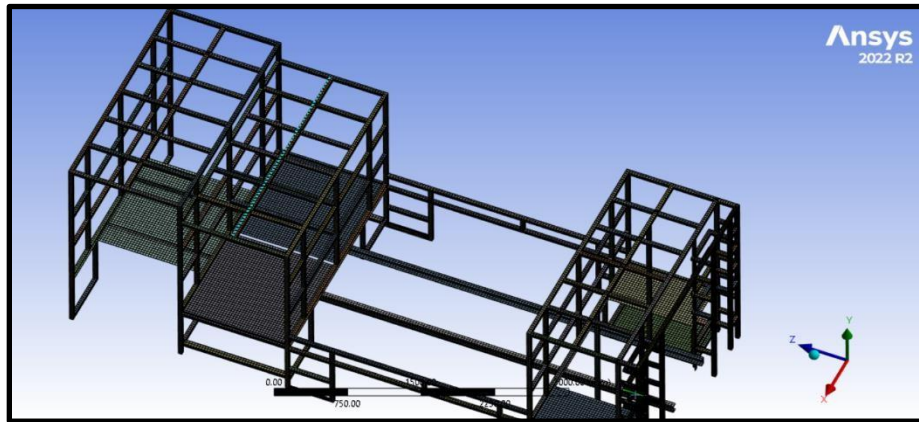


**Figure 5.**

Discretization of the superstructure; global element size 30 mm with local refinements at runner-to-cross-member junctions.

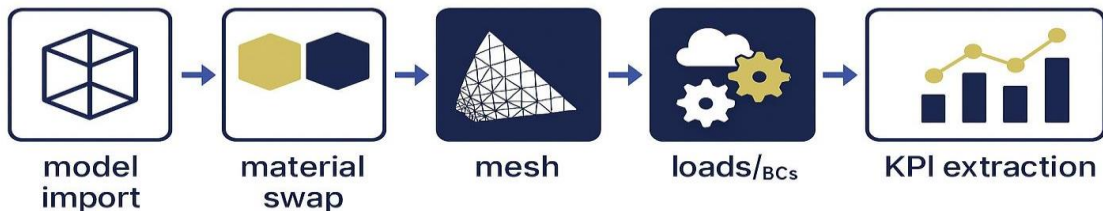
The structural model was analyzed under realistic loading and boundary conditions to simulate operational performance. Continuous fixed support was applied along the underside of the runner channels to represent bolted or welded connections with the chassis side members. The primary load consisted of an 8kL water tank, exerting an overall load of approximately 100,000 N, comprising around 80,000 N from the water mass and 20,000 N from the tank structure transferred through the tank supports onto the runners. Additionally, distributed loads of 500 N were applied at each equipment compartment to represent tools and accessories mounted on shelves. The self-weight of all structural components was inherently accounted for through the assigned material densities.

**Table 3.**

Simulation loads and boundary conditions.

Category	Definition
Supports	Fixed support at runner underside (continuous contact line)
Tank load	100,000 N downward on runner support pads
Compartment loads	500 N per compartment (distributed)
Gravity	Enabled; density per Table 1

Solution settings: Linear static analysis with small-deflection assumption; solver default convergence criteria with strain-energy and force residual checks. For each material case, outputs recorded were total deformation, maximum principal stress, and factor of safety (FoS) using von Mises criteria relative to yield (built-in FoS tool).



**Analysis workflow: model import → material swap → mesh → loads/BCs → solve → KPI extraction.**

**Figure 6.**

Analysis workflow.

### 3.1.2. Performance Metrics (KPIs)

Three primary KPIs were tracked across materials:

**Table 4.**

KPI definitions and interpretation.

KPI	Definition	Engineering purpose
Total Deformation (mm)	Maximum nodal displacement magnitude	Global stiffness measure and serviceability check
Maximum Principal Stress (MPa)	Peak principal stress at any node	Identifies critical regions vs. $\sigma_y$ for yielding risk
Factor of Safety (-)	Allowable/actual stress (vs. yield)	Safety margin and design adequacy indicator

### 3.1.3. Quality Checks and Assumptions

The finite element analysis maintained a high-quality mesh, ensuring that the minimum element quality exceeded the recommended threshold with no inverted elements, while hot-spot stresses at geometric discontinuities were evaluated using standard engineering judgment supported by path plots and averaged stress data where appropriate. Material behavior was assumed to be linear, elastic, and isotropic for the purpose of comparative screening, with nonlinear effects such as plasticity and weld modeling deferred to the prototype validation stage. The tank load was applied as a service-level static load, excluding dynamic amplification factors at this stage, though their inclusion is advised for subsequent fatigue and road load assessments. Geometry, loading, and boundary conditions were kept identical across all material cases to accurately assess material substitution effects.

## 4. Results and Discussion

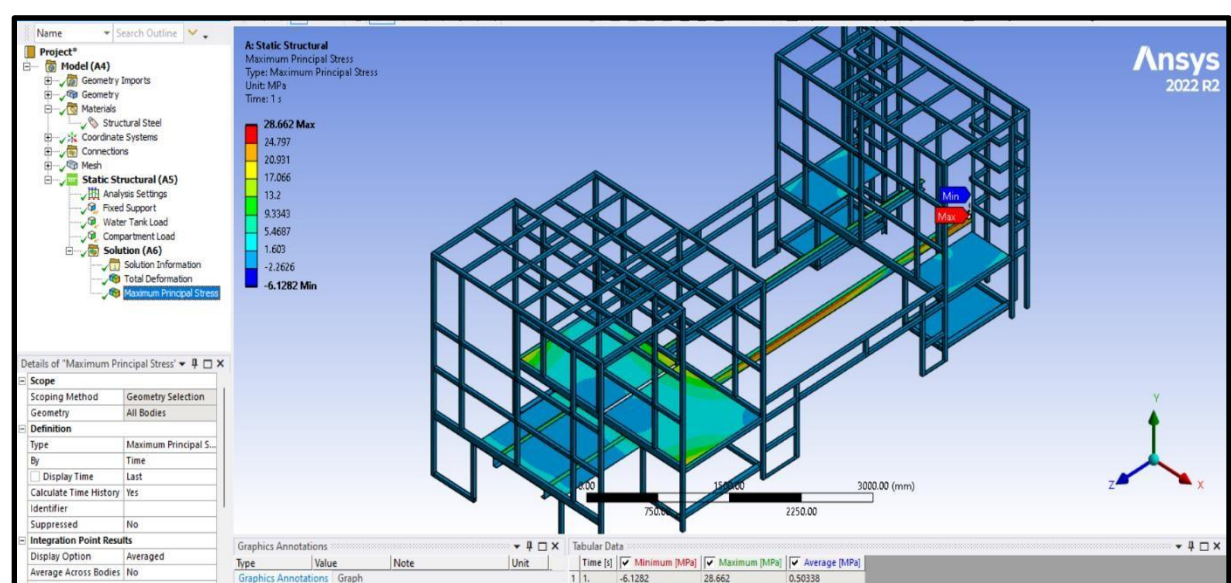
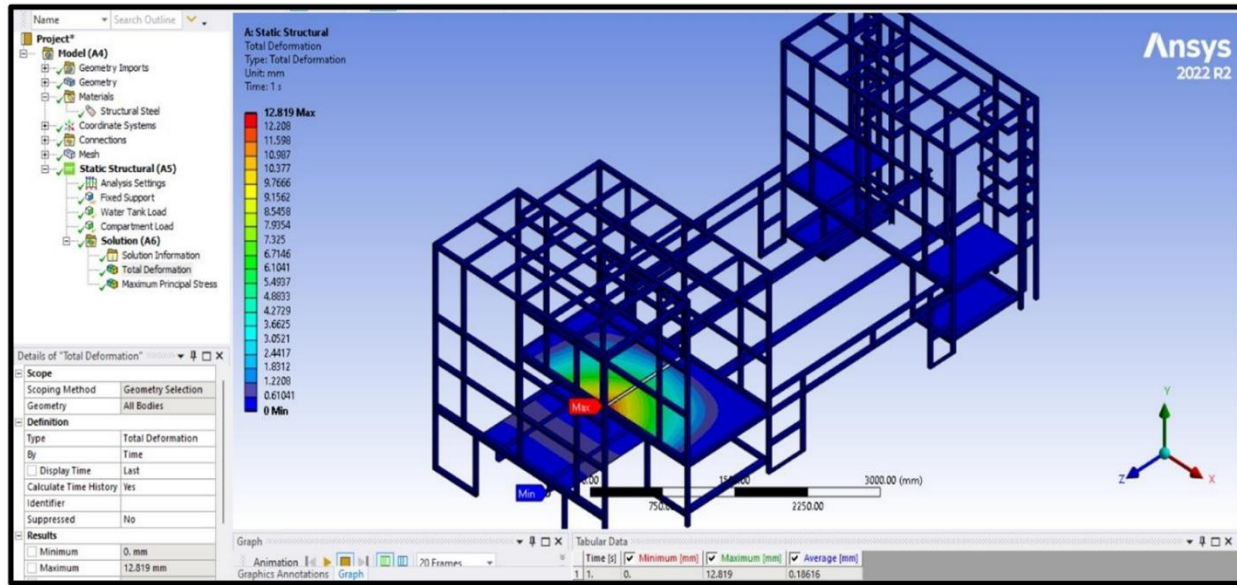
### 4.1. Results

A parametric three-dimensional ladder-frame model of a fire truck was designed using SolidWorks and analyzed through Finite Element Analysis (FEA) in ANSYS under realistic service-based boundary conditions. The study examined the structural performance of three candidate materials, Stainless Steel (SS 304), Mild Steel (IS 2062), and Aluminum Alloy (Al 7075-T6), to determine their suitability for frame construction. Key performance parameters, including maximum and average total deformation, maximum principal stress, and minimum factor of safety (FoS), were evaluated to assess strength and stability. Additionally, the frame mass for each material configuration was derived directly from the CAD model to support a comprehensive comparison of mechanical performance and weight efficiency.

**Table 5.**

Summary of FE results and material metrics

Metric	SS 304	IS 2062 (Mild Steel)	Al 7075-T6
Total deformation (max), mm	13.295	12.81	36.185
Total deformation (avg), mm	0.1925	0.1862	0.5227
Max principal stress, MPa	28.660	28.662	28.653
Yield strength, MPa (ref.)	~292	~460	~500–540
Min FoS (ANSYS)	5.23	6.28	7.16
Frame mass, kg	790	760	300
Indicative material cost, ₹/kg	150–200	60–80	400–500
Notes	Good corrosion resistance; pitting in chlorides	Lowest deformation; economical	Lightest; highest FoS; higher cost



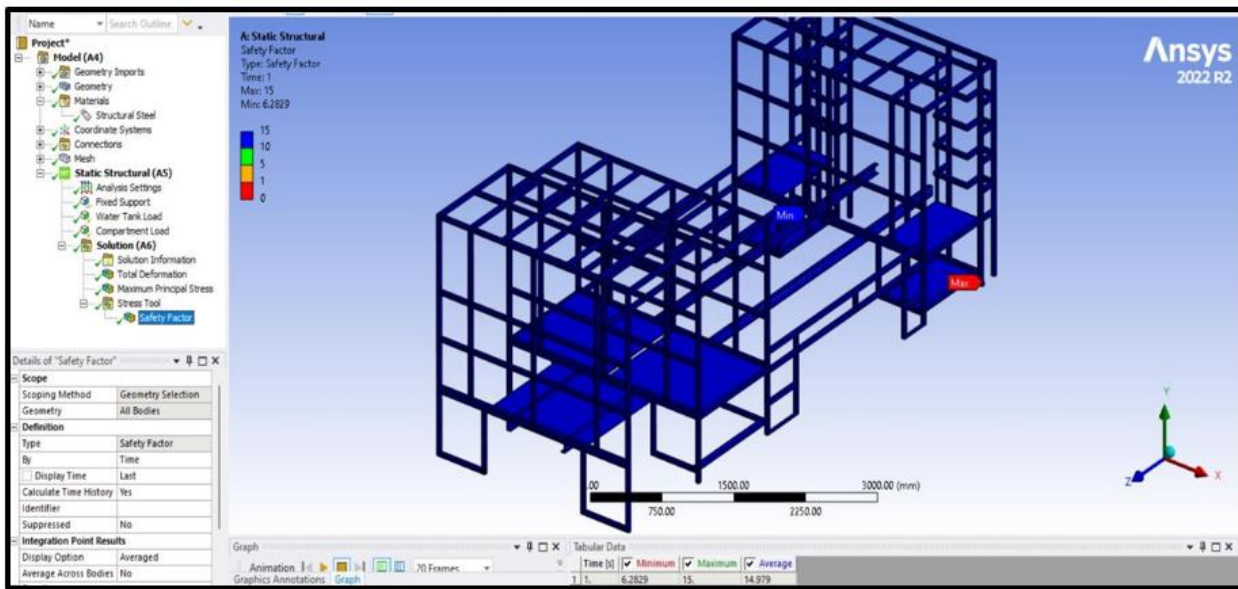


**Figure 9.**  
Factor of Safety map for IS 2062 (ANSYS FoS).

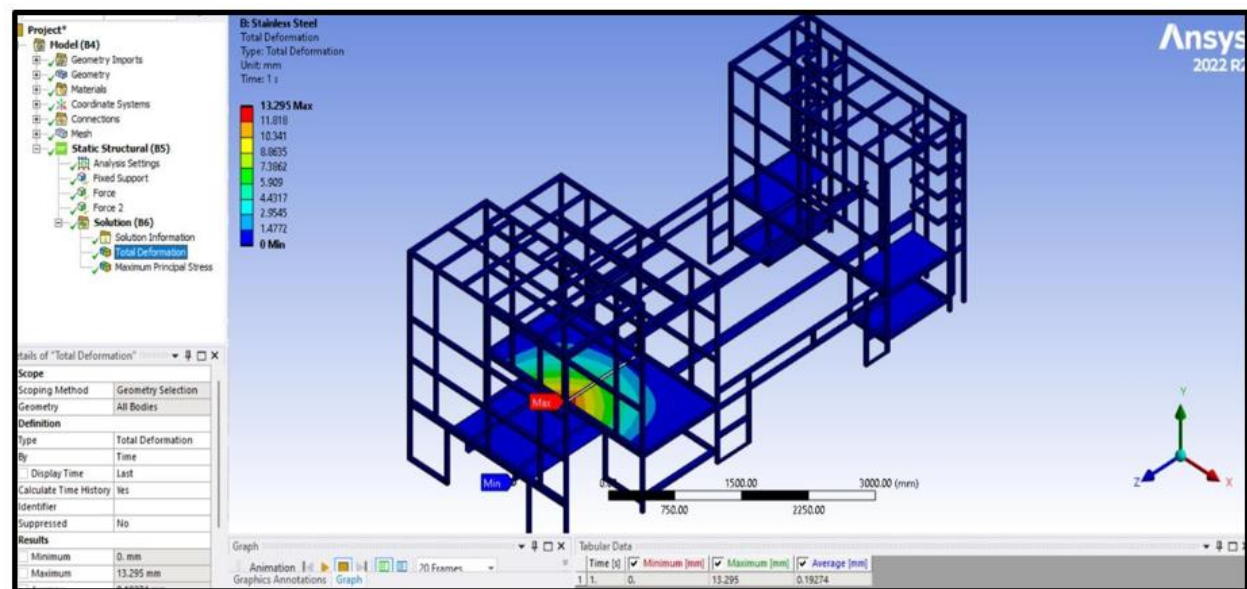


**Figure 10.**  
Total deformation field for SS 304 (mm).

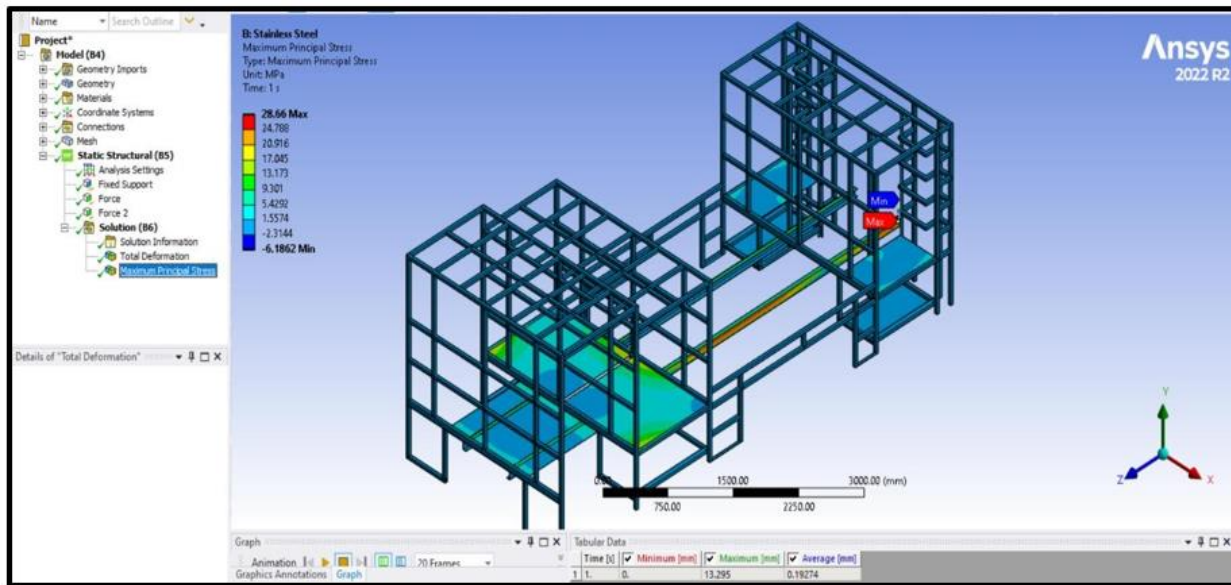


**Figure 11.**  
Maximum principal stress field for SS 304 (MPa).

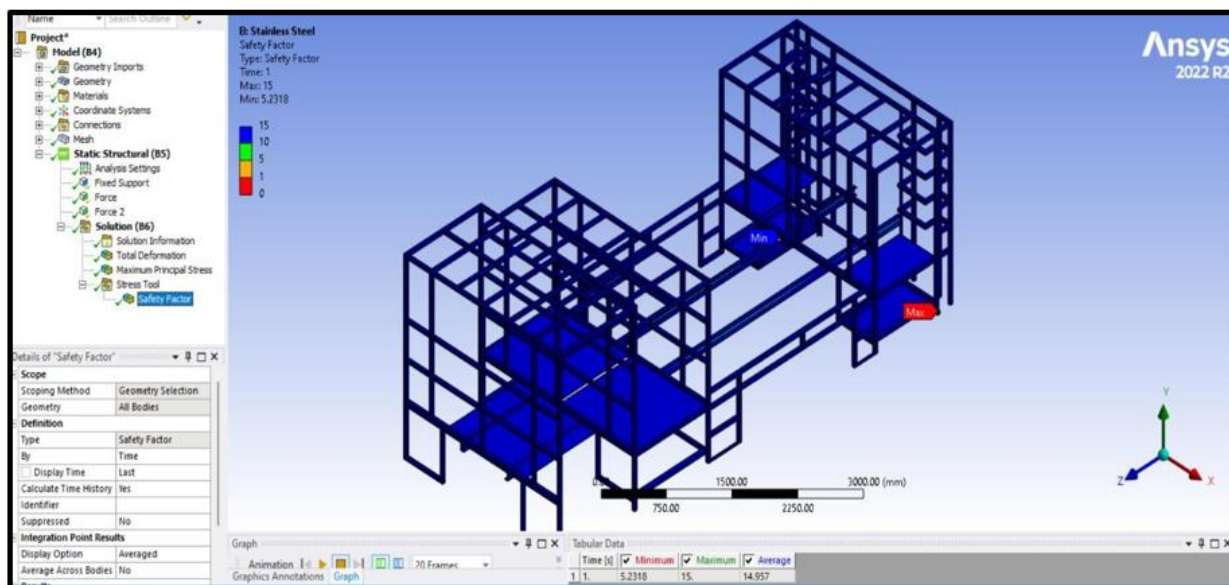


**Figure 12.**  
Factor of Safety (FoS) map for SS 304.

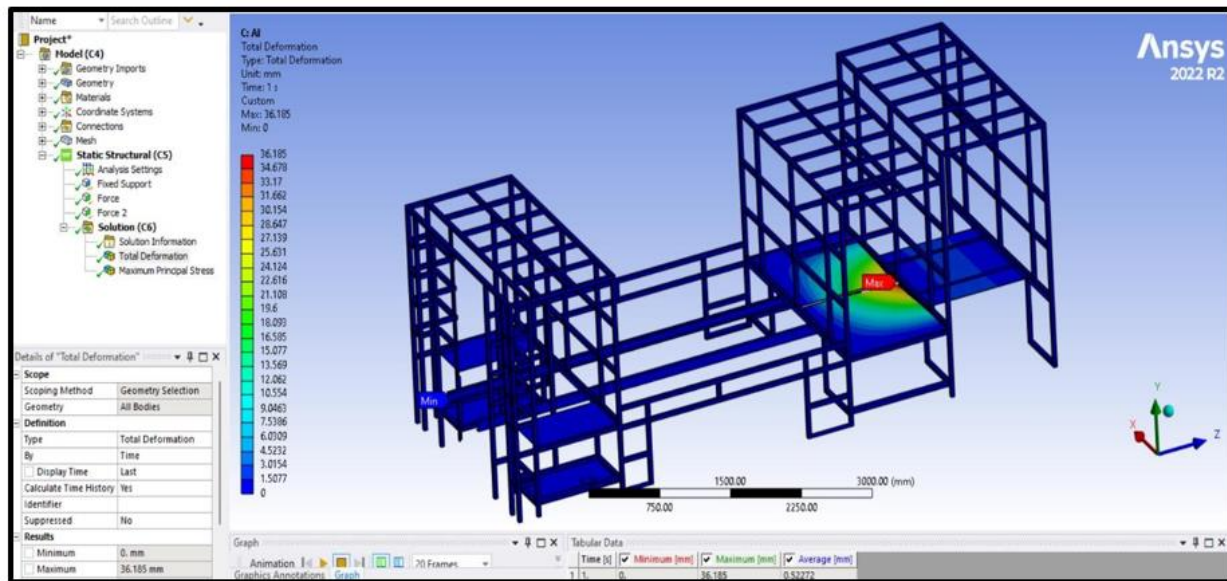


**Figure 13.**  
Total deformation field for Al 7075-T6 (mm).

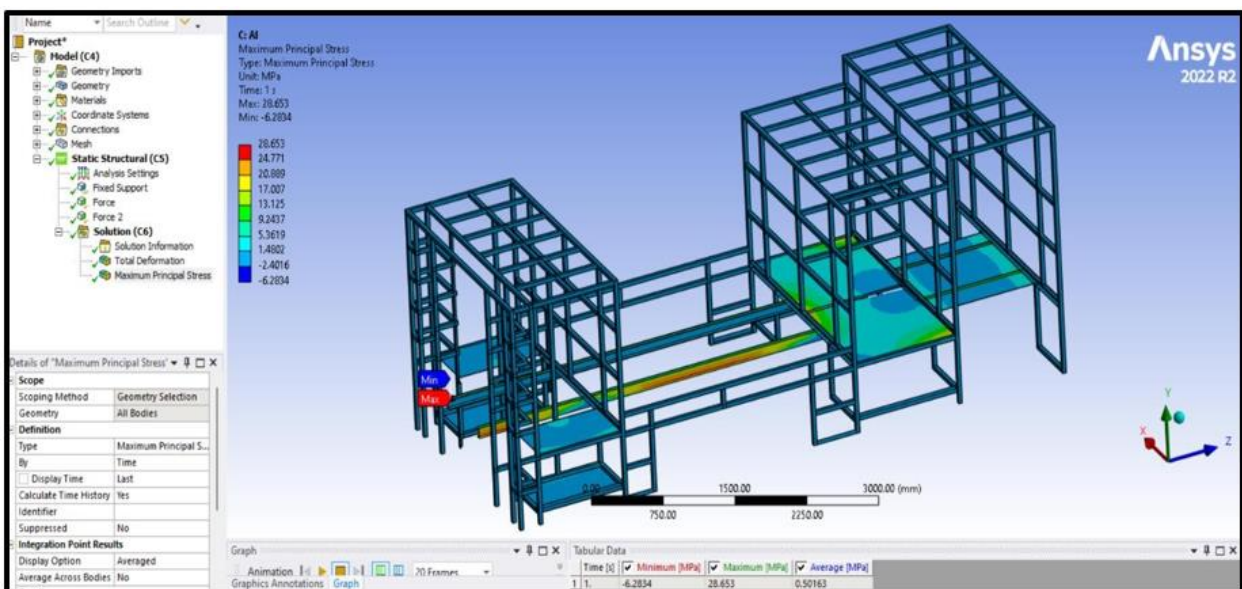


**Figure 14.**  
Maximum principal stress field for Al 7075-T6 (MPa).

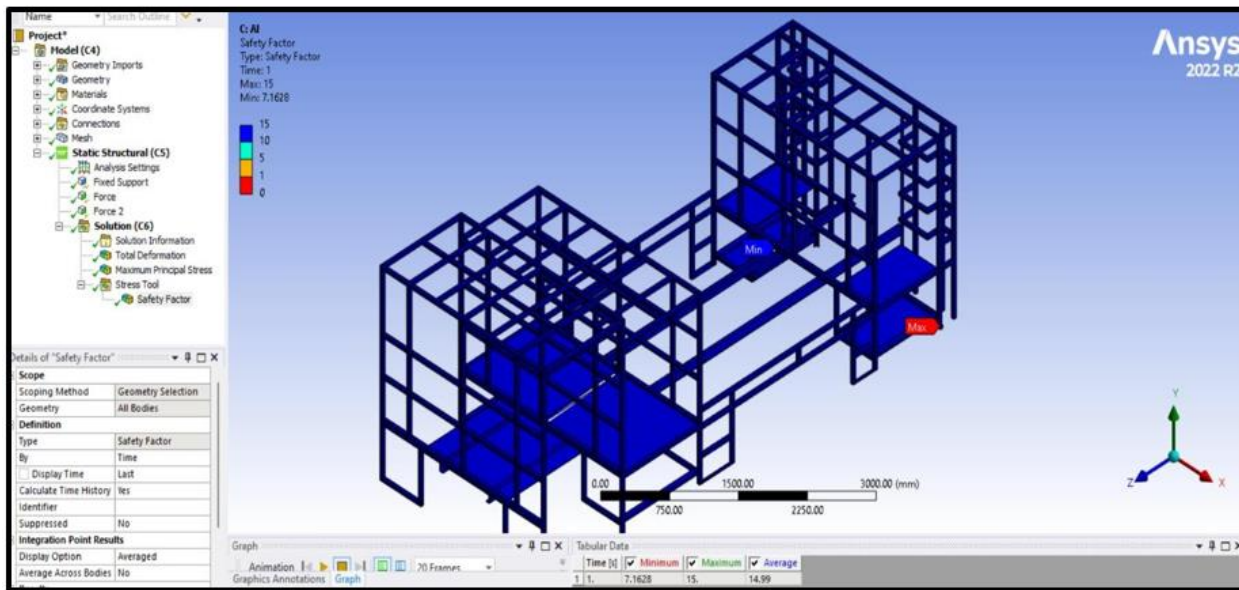


Figure 15.

Factor of Safety (FoS) map for Al 7075-T6.

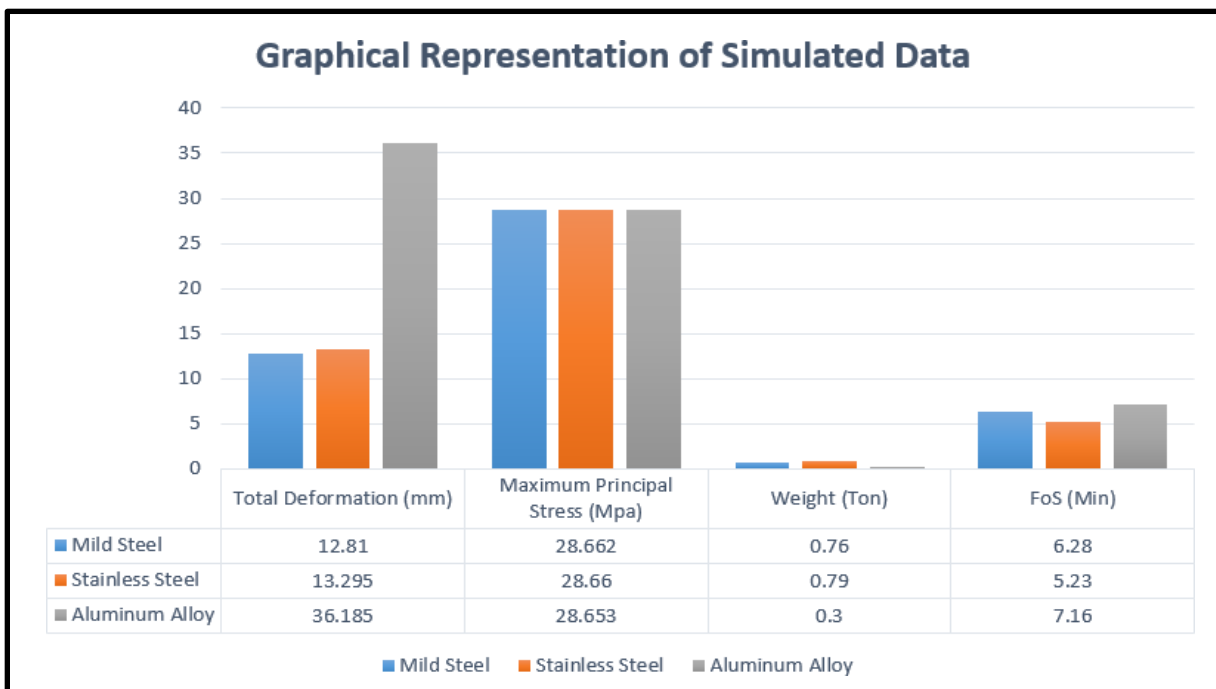


Figure 16.

Comparative plot of key metrics (max deformation, max principal stress, min FoS, and frame mass) for the three materials.

**Table 6.**

Indicative raw-material cost of the frame (from CAD mass  $\times$  mid-price) (Assumptions: SS 175 ₹/kg, MS 70 ₹/kg, Al 450 ₹/kg; for ordering comparisons only).

Material	Mass (kg)	Mid-price (₹/kg)	Indicative cost (₹)
SS 304	790	175	~138,250
IS 2062	760	70	~53,200
Al 7075-T6	300	450	~135,000

**Note:** Prices are market-sensitive; values are illustrative for relative comparison [17].

#### 4.2. Discussion

##### 4.2.1. Deformation and Stiffness

Mild steel exhibited the lowest maximum (12.81 mm) and average (0.186 mm) deformation, followed closely by SS 304 (13.295 mm; 0.193 mm), while Al 7075-T6 showed a larger deformation (36.185 mm; 0.523 mm) yet remained within the design envelope ( $\text{FoS} \geq 7.16$ ). Since geometry and loads are identical, these differences primarily reflect bending stiffness ( $EI$ ), where  $E$  is Young's modulus and  $I$  the section moment of inertia. For a fixed geometry, higher  $E$  lowers deflection; steels ( $E \approx 200\text{--}210 \text{ GPa}$ ) out-stiffen aluminum ( $E \approx 70\text{--}72 \text{ GPa}$ ), explaining aluminum's larger elastic deflections [2]. From a specific stiffness perspective ( $E/\rho$ ), aluminum narrows the gap, which is why, despite higher deflection, it maintains a high  $\text{FoS}$  and offers compelling mass benefits. These trends are consistent with lightweighting literature in heavy vehicles and emergency platforms [1, 10].

##### 4.2.2. Stress Distribution and Margins to Yield

Across all material configurations, the simulations revealed nearly identical maximum principal stresses, averaging around 28.65 MPa. This consistency indicates that the stress distribution was primarily governed by the global load path and boundary conditions, rather than by the inherent material properties of the alloys. The peak stress concentrations appeared predominantly at the runner-overhang junction and near the tank seat region, which are typical zones of high load transfer and limited substructural reinforcement. These results closely correspond with previously reported stress concentration patterns in heavy vehicle chassis systems [10].

A comparative analysis between the observed peak stresses and the nominal yield strengths of the candidate materials further supports the structural integrity of the design. The calculated elastic safety margins were approximately  $10.2\times$  for SS 304 (292 MPa / 28.66 MPa),  $16.1\times$  for IS 2062,

(460 MPa / 28.66 MPa), and  $17.5\times$  for Al 7075-T6 (500 MPa / 28.65 MPa) [13]. Correspondingly, the factor of safety (FoS) fields depicted in Figures 9, 12, and 15 exhibited consistent trends, with minimum FoS values of 5.23 for stainless steel, 6.28 for mild steel, and 7.16 for aluminum alloy, each occurring near geometric discontinuities or constraint points associated with local stress intensifications.

Overall, none of the examined models exhibited yielding under the applied load cases, confirming elastic behavior throughout the structure. The analysis therefore demonstrates that all three materials, SS 304, IS 2062, and Al 7075-T6, offer sufficient strength for the given loading conditions, with aluminum providing the highest safety margin and weight efficiency, making it a promising candidate for lightweight yet structurally sound fire-truck chassis applications.

##### 4.2.3. Fatigue and Durability Considerations

While the present study focuses on quasi-static response, fire truck frames experience variable amplitude loading (accelerations, torsion from uneven terrain, braking loads). Literature indicates aluminum's excellent corrosion resistance and competitive fatigue performance when stress ranges are managed via joint design and weld quality [7, 13]. Steels generally tolerate higher absolute stresses but can be more susceptible to corrosion-assisted fatigue if protection degrades. The FoS levels reported here provide headroom for fatigue design per standard duty cycles; however, a detailed fatigue life assessment (e.g., rain flow counting + S-N curves) is recommended in future work [10,

18].

#### 4.2.4. Mass, Payload, and Energy Implications

The aluminum frame (300 kg) achieves a 62% mass reduction compared to stainless steel (SS) (790 kg), while mild steel trims approximately 3.8%. In operational terms, lower frame mass can either increase payload capacity or reduce fuel consumption. Empirical fleet studies suggest a 6–8% fuel reduction per 10% vehicle-mass reduction [5, 6]. Because a fire truck's total curb mass far exceeds the frame mass, the vehicle-level savings will be lower than the 62% frame-level reduction; nevertheless, the aluminum option offers a materially meaningful path to improved efficiency and reduced emissions, aligning with decarbonization targets for heavy vehicles [1, 10].

#### 4.2.5. Cost, Corrosion, and Manufacturability

Raw-material economics favor mild steel (₹60–80/kg), enabling the lowest indicative frame material cost (Table 5). Aluminum 7075-T6 commands a higher price per kg and can require specialized joining and distortion control in welding or mechanical fastening; however, it offsets these with large mass savings and high FoS [14].

SS 304 offers proven general corrosion resistance, but in chloride-rich coastal environments, the risk of pitting/crevice corrosion increases. For such deployments, SS 316 with Mo additions provides superior pitting resistance and is commonly recommended [1, 9]. Mild steel requires coating systems (e.g., zinc-rich primers + epoxy/polyurethane topcoats) and maintenance discipline to retain durability at low lifecycle cost.

#### 4.2.6. Synthesis and Material Down-Selection

The comparative evaluation of structural materials revealed distinct performance characteristics across mechanical and economic parameters. In terms of stiffness and deflection, mild steel exhibited the least deformation, demonstrating the highest rigidity among all tested materials. Stainless steel (SS 304) closely followed, indicating strong load-bearing capacity under identical boundary conditions. From a strength and safety standpoint, all materials operated well within their elastic limits, confirming structural integrity under the applied load cases. Notably, Al 7075-T6 demonstrated the highest factor of safety (FoS), reflecting superior strength-to-weight performance.

In terms of mass and efficiency, Al 7075-T6 was the lightest, achieving approximately 62% weight reduction compared to SS 304. This substantial decrease in mass directly translates into enhanced payload capacity and improved fuel efficiency, aligning with previous studies [1, 5, 6]. Conversely, mild steel emerged as the most cost-effective option, offering the lowest raw material expenditure while maintaining acceptable performance levels [11].

Environmental durability analysis further highlighted SS 316 as the most suitable material for chloride-rich or marine environments, owing to its excellent resistance to pitting and crevice corrosion. Aluminum alloys, on the other hand, provide broad-spectrum corrosion resistance, making them ideal for general outdoor applications. Mild steel remains a viable candidate when protected by appropriate surface coatings and subjected to regular inspection cycles [12]. Overall, the findings suggest that material selection should balance stiffness, safety, weight efficiency, cost, and environmental exposure, with aluminum alloys offering the best trade-off for lightweight, high-efficiency applications.

Overall, mild steel emerges as a cost-optimal solution with the lowest deflection and ample FoS, well-suited where acquisition cost is paramount. Al 7075-T6 is a premium lightweight alternative with the highest FoS and transformative mass reduction, appropriate where lifecycle performance, payload, or efficiency dominate requirements. SS 304/316 remain viable for high-corrosion contexts, noting mass/cost trade-offs.

## 5. Conclusion

The present study examined the structural performance of fire-truck frame assemblies made from Stainless Steel (SS 304), Mild Steel (IS 2062), and Aluminum Alloy (Al 7075-T6) using a detailed CAD-based finite-element approach. Under identical loading and boundary conditions, all materials showed fully elastic behavior, with the maximum principal stresses ( $\approx 28.6$  MPa) remaining well below their respective yield strengths. Mild steel offered the least deformation (12.81 mm) and the highest rigidity, while the aluminum frame provided the greatest safety margin ( $FoS = 7.16$ ) along with a substantial 62% reduction in mass compared with stainless steel. This reduction has direct implications for improved payload capacity and can yield a 4–5% gain in fuel efficiency for comparable operating conditions. In relative cost terms, aluminum is approximately five to six times more expensive per unit mass than mild steel and about two and a half times higher than stainless steel. Even so, its superior strength-to-weight performance and inherent corrosion resistance make it a strong candidate for modern, lightweight emergency-vehicle designs. Overall, the findings highlight aluminum alloys as the most balanced choice where safety, stiffness, and efficiency must be achieved without compromising structural reliability.

### Transparency:

The authors confirm that the manuscript is an honest, accurate, and transparent account of the study; that no vital features of the study have been omitted; and that any discrepancies from the study as planned have been explained. This study followed all ethical practices during writing.

### Copyright:

© 2025 by the authors. This article is an open-access article distributed under the terms and conditions of the Creative Commons Attribution (CC BY) license (<https://creativecommons.org/licenses/by/4.0/>).

### References

- [1] J. Galos, M. Sutcliffe, D. Cebon, M. Piecyk, and P. Greening, "Reducing the energy consumption of heavy goods vehicles through the application of lightweight trailers: Fleet case studies," *Transportation Research Part D: Transport and Environment*, vol. 41, pp. 40–49, 2015. <https://doi.org/10.1016/j.trd.2015.09.010>
- [2] S. Wang, X. Cui, and L. Zhang, "Lightweight automotive doors design including material and manufacturing process selection," *International Journal of Manufacturing Technology and Management*, vol. 14, no. 1–2, pp. 118–129, 2008. <https://doi.org/10.1504/IJMTM.2008.01749>
- [3] H. C. Kim and T. J. Wallington, "Life cycle assessment of vehicle lightweighting: A physics-based model of mass-induced fuel consumption," *Environmental Science & Technology*, vol. 47, no. 24, pp. 14358–14366, 2013. <https://doi.org/10.1021/es402954w>
- [4] A. Taub, E. De Moor, A. Luo, D. K. Matlock, J. G. Speer, and U. Vaidya, "Materials for automotive lightweighting," *Annual Review of Materials Research*, vol. 49, no. 1, pp. 327–359, 2019. <https://doi.org/10.1146/annurev-matsci-070218-010134>
- [5] G. P. Chirinda and S. Matope, "The lighter the better: Weight reduction in the automotive industry and its impact on fuel consumption and climate change," in *Proceedings of the 2nd African International Conference on Industrial Engineering and Operations Management, Harare, Zimbabwe*, 2020, pp. 7–10.
- [6] J. Sun, "Research on situation and application prospect of automotive body sheets Al-Mg-Si based (6000series) alloy," in *In IOP Conference Series: Materials Science and Engineering (Vol. 452, No. 2, p. 022082)*. IOP Publishing, 2018.
- [7] X. Zheng, Y. Zhang, G.-B. Lou, and Y. Tao, "304D austenitic high-strength stainless steel: High-temperature mechanical properties and fire resistance design for axial compression members," *Structures*, vol. 80, p. 109744, 2025. <https://doi.org/10.1016/j.istruc.2025.109744>
- [8] K. Shanthala, T. Sreenivasa, H. Choudhury, S. Dond, and A. Sharma, "Analytical, numerical and experimental study on joining of aluminium tube to dissimilar steel rods by electro magnetic pulse force," *Journal of Mechanical Science and Technology*, vol. 32, no. 4, pp. 1725–1732, 2018. <https://doi.org/10.1007/s12206-018-0328-0>
- [9] P. A. G. Piloto, L. M. R. Mesquita, Á. A. T. Cruz, N. Lopes, F. Arrais, and P. V. Real, "Bending resistance of austenitic stainless steel hollow sections at elevated temperatures," *Structures*, vol. 59, p. 105690, 2024. <https://doi.org/10.1016/j.istruc.2023.105690>

- [10] S. Padmanabhan, S. C. Undamatla, and H. V. Reddy, "Investigation of material impact on Truck frame design through Structural Analysis," in *IOP Conference Series: Materials Science and Engineering* (Vol. 923, No. 1, p. 012011). *IOP Publishing*, 2020.
- [11] A. Agarwal and L. Mthembu, "FE design analysis and optimization of heavy-duty truck chassis using sparse grid initialization technique," *Materials Today: Proceedings*, vol. 60, pp. 2084-2092, 2022. <https://doi.org/10.1016/j.matpr.2022.01.471>
- [12] A. Agarwal and L. Mthembu, "Weight optimization of heavy-duty truck chassis by optimal space fill design using light weight Graphite Al GA 7-230 MMC," *Materials Today: Proceedings*, vol. 52, pp. 1278-1287, 2022. <https://doi.org/10.1016/j.matpr.2021.11.053>
- [13] D. Dhablya, A. Alkkhayat, J. Sivakumar, and R. Bhokde, "Design and analysis of four-wheeler chassis for improved performance," in *2023 4th International Conference on Computation, Automation and Knowledge Management (ICCAKM)* (pp. 1-8). *IEEE*, 2023.
- [14] S. Li, X. Yang, J. Wang, Y. Wang, and C. Guo, "Finite element analysis and optimization design of the frame of heavy-duty trucks," *International Journal of Mechatronics and Applied Mechanics*, vol. 1, no. 20, pp. 40-46, 2025. <https://doi.org/10.17683/ijomam/issue20.4>
- [15] M. Tisza, "High strength steels and aluminium alloys in lightweight body manufacturing," *Archives of Materials Science and Engineering*, vol. 88, no. 2, pp. 68-74, 2017. <https://doi.org/10.5604/01.3001.0010.8041>
- [16] R. Wohlecker and R. Henn, "Mass reduction potential of steel and aluminum in automotive applications," *SAE International Journal of Materials and Manufacturing*, vol. 1, no. 1, pp. 480-484, 2009. <https://doi.org/10.4271/2008-01-1078>
- [17] J. Cheng, K. Liu, S. Shao, and P. Cheng, "Research on the impact of iron ore price fluctuations on the steel industry output," *China Mining Magazine*, vol. 34, no. 2, pp. 212-221, 2025. <https://doi.org/10.12075/j.issn.1004-4051.20242156>
- [18] X. Zhang *et al.*, "Mechanism investigation on fatigue failure in threaded hole of the main bearing in high-strength diesel engine," *Engineering Failure Analysis*, vol. 143, p. 106921, 2023. <https://doi.org/10.1016/j.engfailanal.2022.106921>